Electrically tuneable lateral leakage loss in liquid crystal clad shallow-etched silicon waveguides

Thomas Ako,[1,2,*] **Anthony Hope,**[2,3,4] **Thach Nguyen,**[4] **Arnan Mitchell,**[4] **Wim Bogaerts,**[2,3] **Kristiaan Neyts,**[1,2] **and Jeroen Beeckman**[1,2]

[1]*Liquid Crystals and Photonics Group, Department of Electronics and Information Systems, Ghent University, St. Pietersnieuwstraat 41, 9000 Ghent, Belgium*

[2]*Center for Nano- and Bio-Photonics, Ghent University, St. Pietersnieuwstraat 41, 9000 Ghent, Belgium*

[3]*Photonics Research Group, Department of Information Technology, Ghent University, St. Pietersnieuwstraat 41, 9000 Ghent, Belgium*

[4]*ARC Center of Excellence for Ultrahigh Bandwidth Devices for Optical Systems (CUDOS) and School of Electrical and Computer Engineering, RMIT University, Melbourne, Australia*

[*]*thomas.ako@elis.ugent.be*

Abstract: We demonstrate electrical tuning of the lateral leakage loss of TM-like modes in nematic liquid crystal (LC) clad shallow-etched Silicon-on-Insulator (SOI) waveguides. The refractive index of the LC layer can be modulated by applying a voltage over it. This results in a modulation of the effective index of the SOI waveguide modes. Since the leakage loss is linked to these effective indices, tunable leakage loss of the waveguides is achieved. We switch the wavelength at which the minimum in leakage loss occurs by 39.5nm (from 1564nm to 1524.5nm) in a 785nm wide waveguide. We show that the leakage loss in this waveguide can either be increased or decreased by modulating the refractive index of the LC cladding at a fixed wavelength.

References and links

1. M. Heck, H.-W. Chen, A. Fang, B. Koch, D. Liang, H. Park, M. Sysak, and J. Bowers, "Hybrid silicon photonics for optical interconnects," IEEE J. Sel. Top. Quantum Electron. **17**, 333–346 (2011).
2. J. Doylend and A. Knights, "The evolution of silicon photonics as an enabling technology for optical interconnection," Laser Photon. Rev. **6**, 504–525 (2012).
3. P. Dong, W. Qian, S. Liao, H. Liang, C. Kung, N. Feng, R. Shafiiha, J. Fong, D. Feng, A. Krishnamoorthy, and M. Asghari, "Low loss shallow-ridge silicon waveguides," Opt. Express **18**, 14474–14479 (2010).
4. S. K. Selvaraja, W. Bogaerts, P. Absil, D. Van Thourhout, and R. Baets, "Record low-loss hybrid rib/wire waveguides for silicon photonic circuits," in "Group IV Photonics, 7th International conference, Proceedings," (IEEE, 2010), p. 3.
5. M. Webster, R. Pafchek, A. Mitchell, and T. Koch, "Width dependence of inherent tm-mode lateral leakage loss in silicon-on-insulator ridge waveguides," IEEE Photon. Technol. Lett. **19**, 429–431 (2007).
6. R. Pafchek, R. Tummidi, J. Li, M. Webster, E. Chen, and T. Koch, "Low-loss silicon-on-insulator shallow-ridge te and tm waveguides formed using thermal oxidation," Appl. Opt. **48**, 958–963 (2009).
7. T. Nguyen, R. Tummidi, T. Koch, and A. Mitchell, "Lateral leakage of tm-like mode in thin-ridge silicon-on-insulator bent waveguides and ring resonators," Opt. Express **18** (2010).
8. M. Koshiba, K. Kakihara, and K. Saitoh, "Reduced lateral leakage losses in tm-like modes in silicon-on-insulator ridge waveguides," Opt. Lett. **33**, 2008–2010 (2008).

9. K. Kakihara, K. Saitoh, and M. Koshiba, "Generalized simple theory for estimating lateral leakage loss behavior in silicon-on-insulator ridge waveguides," J. Lightwave Technol. **27**, 5492–5499 (2009).
10. N. Dalvand, T. Nguyen, R. Tummidi, T. Koch, and A. Mitchell, "Thin-ridge silicon-on-insulator waveguides with directional control of lateral leakage radiation," Opt. Express **19**, 5635–5643 (2011).
11. T. Nguyen, R. Tummidi, T. Koch, and A. Mitchell, "Rigorous modeling of lateral leakage loss in soi thin-ridge waveguides and couplers," IEEE Photon. Technol. Lett. **21**, 486–488 (2009).
12. T. Ako, J. Beeckman, W. Bogaerts, and K. Neyts, "Tuning the lateral leakage loss of tm-like modes in shallow-etched waveguides using liquid crystals," Appl. Opt. **53**, 214–220 (2014).
13. W. Cort, J. Beeckman, R. James, F. Fernandez, R. Baets, and K. Neyts, "Tuning of silicon-on-insulator ring resonators with liquid crystal cladding using the longitudinal field component," Opt. Lett. **34**, 2054–2056 (2009).
14. W. Cort, J. Beeckman, T. Claes, K. Neyts, and R. Baets, "Wide tuning of silicon-on-insulator ring resonators with a liquid crystal cladding," Opt. Lett. **36**, 3876–3878 (2011).
15. V. G. Chigrinov, "Photoaligning and photopatterning a new challenge in liquid crystal photonics," Crystals **3**, 149–162 (2013).
16. J. Li, S.-T. Wu, S. Brugioni, R. Meucci, and S. Faetti, "Infrared refractive indices of liquid crystals," J. Appl. Phys. **97**, 073501 (2005).
17. H. Desmet, K. Neyts, and R. Baets, "Modeling nematic liquid crystals in the neighborhood of edges," J. Appl. Phys. **98**, 123517 (2005).
18. N. Dalvand, T. Nguyen, T. Koch, and A. Mitchell, "Thin shallow-ridge silicon-on-insulator waveguide transitions and tapers," IEEE Photon. Technol. Lett. **25**, 163–166 (2013).

1. Introduction

In recent years, Silicon-on-Insulator (SOI) photonics has successfully established itself as a viable technology for photonic integrated circuits, especially for optical interconnect applications [1, 2]. This success is in large part due to intrinsic advantages which arise as a result of working within the SOI material platform: the high index contrast makes it feasible to design waveguides with very narrow bends, making high density integration a practical reality. In addition to this, compatibility with existing complementary metal-oxide semiconductor (CMOS) fabrication facilities means SOI photonics isn't impeded by expensive start up costs. The two main types of waveguides used in SOI technology are deep-etched (strip/wire) and shallow-etched (ridge) waveguides. Propagation losses of 0.27dB/cm and 1 to 2dB/cm have been reported for shallow-etched and deep-etched waveguides respectively [3, 4]. This indicates that shallow-etched waveguides are suitable for applications where an optical signal needs to be efficiently transmitted over a distance of a few tens of centimeters e.g. on-chip optical interconnects. Due to their geometry, shallow-etched waveguides also allow lateral electrical access; this makes them suitable for active devices like waveguide modulators and lasers.

Because of their high index contrast, silicon waveguides are extremely birefringent: the TE-like mode and the TM-like mode have very different propagation constants. Therefore, silicon waveguides are usually used only for the TE polarization. Strip waveguides also guide TM-polarized light, but in shallow-etched waveguides, it has been theoretically and experimentally demonstrated that the TM-like mode suffers from waveguide-width-dependent lateral leakage loss [5, 6]. The effective index of the guided TM-like mode in such waveguides is comparable to that of the radiating (cladding) slab TE-like mode. This radiating slab TE-like mode can propagate in any direction since it is unguided and can be phase matched to the guided TM-like mode at a particular angle. The guided TM mode thus suffers from lateral leakage loss since it can be phase matched to a radiating mode. Accordingly, the TM-like mode in a shallow-etched waveguide is always lossy except for the case when the waveguide satisfies the well known resonance condition [5].

$$W = \frac{m\lambda}{\sqrt{n_{eff,TE}^{(core)}{}^2 - N_{eff,TM}^2}} \tag{1}$$

Where W is the waveguide width, λ is the wavelength of the light in vacuum, m is a positive integer denoting the order of the resonance condition, $N_{eff,TM}$ is the effective index of the guided TM-like waveguide mode and $n_{eff,TE}^{(core)}$ is the effective index of the (unguided) TE wave which traverses the waveguide core. Conversely, for a waveguide with a fixed width, there exists a wavelength at which the leakage loss is minimal.

In addition to straight waveguides, this lateral leakage behavior has been reported to be present in shallow-etched bent waveguides and ring resonators [7] as well. Several attempts have been made to mitigate this undesirable effect [8–10]. In the current work , we propose a method for actively tuning the position of the leakage loss minima in liquid crystal (LC) clad shallow-etched waveguides by applying a voltage over the LC.

The silicon devices were designed using the IPKISS parametric design framework and fabricated by IMEC through the ePIXfab multi-project-wafer service. They consist of a 220nm silicon layer on a 2μm buried oxide layer. The grating couplers and the shallow-etched waveguides are defined by a 70nm etch into the silicon, while the other waveguide structures (such as the grating coupler tapers) are fully etched. For our experiments we did not have an oxide cladding deposited, so the top silicon surface is exposed to air. Figure 1 shows a sketch of the geometry of the waveguide and the coordinate system we use.
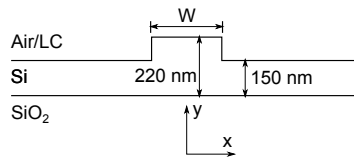

Fig. 1. Geometry of a shallow-etched SOI waveguide. The z-axis is perpendicular to the plane of the paper.

We design the waveguides to be 1 cm long with varying widths. The widths of the waveguides are chosen so that they are close to the first leakage loss minimum in the desired wavelength range as expected from previous theoretical considerations [5, 7, 11, 12]. The waveguides have grating couplers placed at their extremities. The grating couplers are optimized for TM polarized light. They are curved and have a period of 1050nm with a fill factor of 50%. Light is coupled into and out of the waveguides by placing optical fibers inclined at an angle of $10°$ with the vertical above the grating couplers.

The remainder of the paper is organized as follows. In Section 2, we present measurements of the leakage loss of air-clad waveguides and compare them to previous results reported in the literature. Section 3 is devoted to the study of LC clad waveguides. Here we give all details concerning the assembly of the LC cladding over the shallow-etched waveguides. Section 4 deals with a discussion of the phenomenology uncovered by the experiments we perform. We conclude the paper in Section 5.

2. Air cladding

The purpose of the air-clad measurements is two-fold. First, we need to ensure that the waveguides we work with exhibit the leakage loss behavior as expected. Second, we intend to study the potentially complicated effect a LC cladding has on the leakage properties of a waveguide. Accordingly, a measurement of the air-clad case provides a bench mark for the more complicated case. We focus on the wavelength window from 1510nm to 1590nm which is determined by the experimental setup.

A loss measurement is carried out as follows; we use a fiber-coupled tuneable laser to couple light into the shallow-etched waveguide through one grating coupler. The light is coupled out of
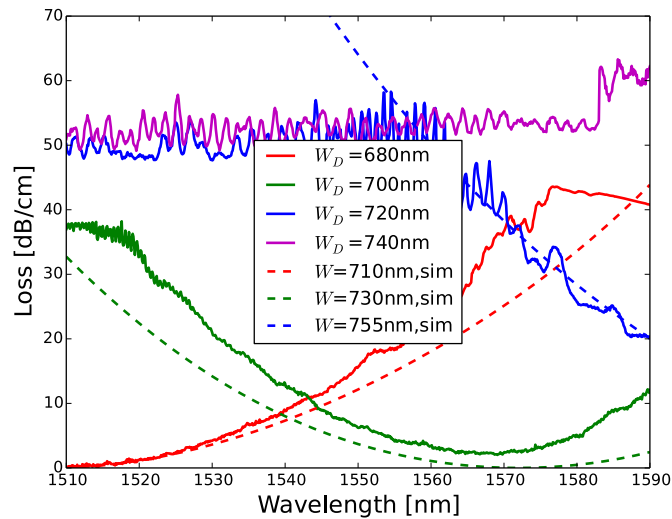
Fig. 2. Variation of the loss with wavelength for an air-clad shallow-etched silicon waveguide. Solid curves: experimental data. Dashed curves: simulation data.

the waveguide at the other grating coupler into a fiber-coupled power meter. Each measurement is corrected for the contribution of the grating couplers by subtracting the transmission of a short deep-etched waveguide with identical grating couplers at its extremities. The variation of the loss as a function of the wavelength for four different waveguide widths has been plotted in Fig. 2. Overall, we see excellent agreement between measurement and simulation. We did observe a discrepancy between the designed waveguide width (W_D) and the actual waveguide width (W). The waveguides are designed to be 680nm, 700nm and 720nm wide but are found to actually be 710nm, 730nm and 755nm wide respectively. This is confirmed by SEM measurements.

3. Liquid crystal cladding

3.1. Device fabrication

We now turn our attention to LC clad waveguides. In order to facilitate the deposition of a uniform LC layer on the waveguides, a LC cell is assembled based on the technology used in LC display research [13]. The cell consists of an SOI chip (on which the waveguides are lithographically defined) and a glass plate [14]. Since the waveguides are 1cm long, the glass plate is cut so that it is 7mm wide. As such it is possible to cover the waveguides and still leave the grating couplers in air for easy coupling of light in and out of the waveguides. The glass plate has a thin layer of indium tin oxide (ITO) deposited on it. The ITO is transparent and acts as the top electrode of the cell while the silicon substrate is the bottom electrode. Accurately controlling the alignment of the LC over the waveguides is very important for the proper operation of our device. The photo-alignment [15] method is an excellent candidate for aligning the LC on top of the waveguides. It possesses many advantages over the rubbing alignment method. Tests were performed with a photo-alignment layer deposited on top of the waveguides. The material was illuminated with UV light. This resulted in LC being aligned parallel to the waveguides. However, measurements revealed that the loss of the waveguides with photo-aligned LC was too high and it was impossible to resolve minima in leakage loss. This is not very surprising given the leaky nature of the TM polarized waveguide modes. Consequently, we resorted to using

the rubbing alignment method. A 2.5μm thick poly methyl methacrylate (PMMA) layer is spin coated on the ITO. It ensures that the vertical separation between the ITO and the waveguide is large enough to prevent light absorption. In order to preferentially align the director of the LC molecules in a given direction, a thin nylon alignment layer is spin coated onto the PMMA layer. The alignment layer is then rubbed with a soft cloth and forces the LC molecules to align in a planar manner in the direction of the rubbing, with a pretilt of about 2° with the z-axis. We choose the rubbing direction to be parallel to the waveguides on the SOI chip. The glass plate and the SOI chip are glued together with UV curable glue mixed with silica spacer balls. The diameter of the spacer balls determines the thickness of the gap between the glass plate and the chip. Wires are soldered to the ITO on the glass plate and the silicon substrate; this makes it possible to apply a voltage over the LC layer in the cell. The cell is filled with the commercially available LC E7 (ordinary index (n_o) = 1.5024 and extraordinary index (n_e) = 1.697 at 1550nm [16]) by capillary action. For thin cells, the filling must be performed in vacuum in order to avoid the formation of air bubbles in the cell. A schematic of the fully assembled cell is shown in Fig. 3.
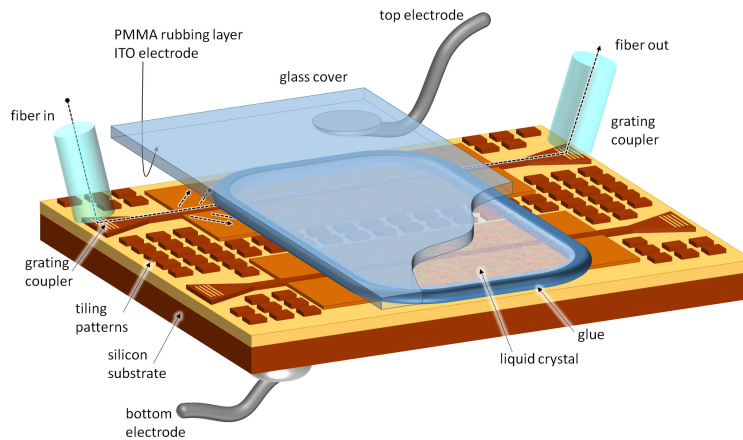

Fig. 3. Schematic of the cell

3.2. *Liquid crystal switching behavior*

The alignment of the LC is critical to the performance of our device. If the LC molecules covering the waveguides are not well aligned, several domains and dis-inclinations are formed. Light propagating through such a LC layer is scattered at the domain boundaries. Given that lateral leakage loss occurs at the side walls of the waveguides, this scattering will increase the overall loss from the waveguides; making the observation of the lateral leakage loss difficult. Conversely, if the LC molecules covering the waveguides are perfectly aligned, the layer has a well defined director. In this case, the lateral leakage loss should be easier to measure since the scattering by a well aligned LC layer should be negligible.

Figure 4 shows the cell placed in a polarization microscope under crossed polarizers in reflection mode. For zero applied voltage (Fig. 4(a)), we observe that the LC close to the waveguides is well aligned (dark areas) whereas defects form at the edge of the side cladding which are patterned with period structures for pattern density control. The rubbing of the alignment layer on the glass plate is parallel to the waveguides. The LC molecules close to the glass plate align themselves following the rubbing. Close to the waveguides the LC molecules find it energetically favourable to align themselves with their long axes parallel to the waveguides [17]. This
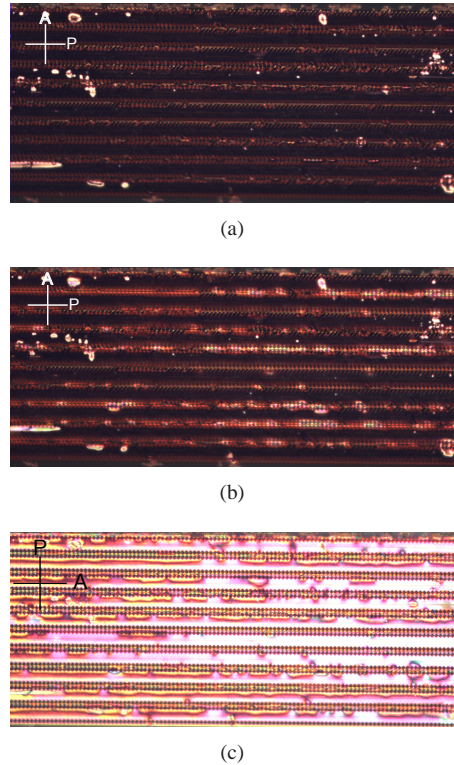
Fig. 4. LC cell under crossed polarizers in reflection microscopy with lines showing the orientation of the polarizer (P) and analyzer (A). (a) 0Vpp (b) 40Vpp, onset of switching in the LC cell (c) 80Vpp.

results in a uniform alignment in this area of the LC layer. At the side of the etched cladding, the LC molecules are twisted (both left-handed and right-handed) by the periodic structures. Hence we have defects forming over the sides. As the voltage over the LC layer is increased, the defects formed at the sides grow and propagate throughout the cell. Figure 4(b) shows the onset of the LC switching in the cell. For higher applied voltages as in Fig. 4(c) we notice that the defects can propagate towards the waveguides, causing the well aligned part of the LC there to shrink. We can see a different domain boundaries between regions with different alignment in between the waveguides.

The thickness of the LC cladding has a strong effect on the overall loss of the waveguides. Measurements for different LC layer thicknesses reveal that a thin LC layer results in less defects. Since we have a 2.5μm thick PMMA layer on the top glass plate, we can have a thin LC layer and still avoid absorption by the ITO. We fix the thickness of the LC layer in the cell at 5.6μm. All results presented further on in this work are for such a cell.

3.3. Tunable leakage loss measurements

We now turn our attention to lateral leakage loss measurements of the LC clad waveguides. The waveguide modes now feel either n_o or n_e in the cladding. This means that the effective indices of the waveguide modes increase compared to the air-clad case. Because of the different orientation of the dominant E-field in the TE and TM modes, the increase in $N_{eff,TM}$ is higher than that in $n_{eff,TE}^{(core)}$. However, $n_{eff,TE}^{(core)}$ is still larger than $N_{eff,TM}$, hence the numerator in (1)

decreases. Accordingly, the wavelength at which the minimum in leakage loss occurs (magic wavelength) shifts to shorter wavelengths as depicted in Fig. 5.
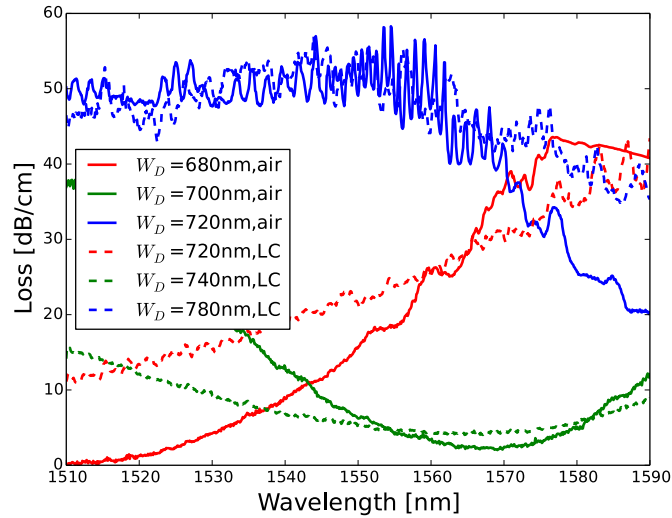

Fig. 5. Comparison of the variation of loss with wavelength for air and LC clad (for 0Vpp) shallow etched SOI waveguides.

We note from Fig. 5 that the leakage loss exhibited in air-clad waveguides is preserved in the LC clad waveguides. The waveguide with $W_D = 740$nm is interesting since it exhibits its magic wavelength within the wavelength window of interest. The leakage loss variation of the other waveguides (with different width) indicate that their magic wavelength lies at shorter ($W_D = 720$nm) and longer ($W_D = 780$nm) wavelengths respectively. We have modeled these LC clad waveguides and found good agreement between our simulations and the measurements as depicted in Fig. 6(a). Note that the theoretical loss minimum is 0dB/cm which is obviously not the case in the practice. The waveguides designed to be 720nm and 740nm wide are found to correspond to 750nm and 785nm wide waveguides respectively. In order to determine the range over which the magic wavelength can be tuned, we model the 5.6μm thick cladding layer as a uniaxial material with c-axis along the z (green dashed curve) and y (black dashed curve) axes respectively. With the former and latter being the initial and final states of our LC cladding. Figure 6(b) shows a plot of the E-field components in the waveguide. Notice that in the area occupied by the LC in the cell (y distance greater than 0.11μm), the y component is stronger than the z component. Accordingly, the position of the magic wavelength can be switched by more than 70nm by reorienting the LCs in the cladding from being aligned along the z axis to being aligned along the y-axis (see Fig. 6(a)).

The tuning of the leakage loss behavior is achieved by applying a voltage over the LC cladding. This causes the LC molecules to reorient themselves so that they are more and more parallel with the electric field lines (along the y-axis). The index felt by the TM-like mode in the upper cladding is given by;

$$n_{clad} = \frac{1}{\sqrt{(\frac{\cos\alpha}{n_o})^2 + (\frac{\sin\alpha}{n_e})^2}} \tag{2}$$

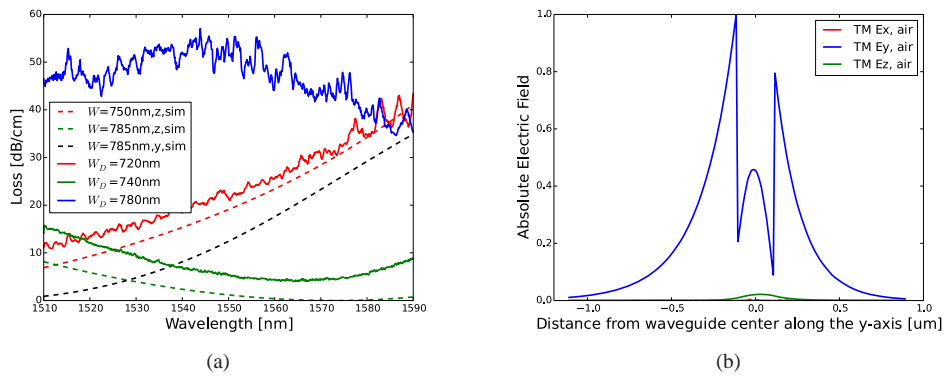with α the angle the LC director makes with the z-axis. For zero applied voltage, $\alpha = 0$. α

Fig. 6. (a)Simulated versus measured loss values for LC clad waveguides. Solid lines: measured lateral leakage loss data. Dashed lines: simulation data. Dark dashed line: y-aligned cladding. (b)Field profiles of the various E-field components for a $W = 785$nm waveguide with air cladding. Notice that the y component is much stronger than the z component in the area (y distance greater than 0.11μm) occupied by the LC.

increases with increasing applied voltage attaining its maximum value of $90°$ for high applied voltages. Accordingly, $n_{clad} \sim n_o$ for low voltages and $n_{clad} \sim n_e$ for high voltages. The applied voltage is swept from 0Vpp to 300Vpp in steps of 20Vpp. For each voltage step, we measure the leakage loss over the wavelengths ranging from 1510nm to 1590nm. We plot the result of these measurements for the 785nm wide ($W_D = 740$nm) waveguide in Fig. 7(a). As the voltage is increased, the wavelength at which the minimum in leakage loss occurs shifts to shorter wavelengths. We measure a shift from 1564nm at 0Vpp to 1524.5nm at 300Vpp; this is about 56 % of the change predicted from simulations for perfectly aligned LC cladding layers. We also notice that the shift in the wavelength at which the minimum in leakage loss occurs is accompanied by an increase in loss. On average the loss in the waveguide increases by about 8dB/cm when the voltage is changed from 0Vpp to 300Vpp.
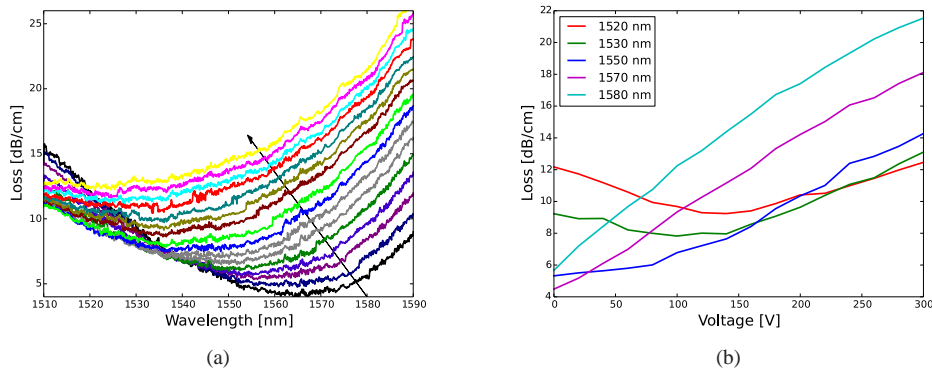

Fig. 7. (a)Voltage tuning of the loss in a $W_D = 740$nm wide LC clad waveguide. The voltage is ramped from 0Vpp (black) to 300Vpp (yellow) in steps of 20Vpp. The arrow indicates the direction in which the loss curve shifts when the applied voltage is increased. (b)Voltage dependence of the lateral leakage loss in a $W_D = 740$nm LC clad waveguide.

We complete this section by taking a look at the voltage dependence of the leakage loss of the LC clad waveguide. Figure 7(b) shows plots of this dependency for five different wavelengths. For 1550nm, 1570nm, and 1580nm, the leakage loss increases with increasing voltage. For example at 1570nm the loss increases from 4.5dB/cm at 0Vpp to 18.1dB/cm at 300Vpp. Whereas at 1580nm the loss increases from 5.7dB/cm at 0Vpp to 21.5dB/cm at 300Vpp. For 1520nm and 1530nm, the loss decreases with increasing voltage but as the voltage increases past a certain point, it increases again. For example at a wavelength of 1520nm, the leakage loss decreases from 12.2dB/cm at 0Vpp to 9.2dB/cm at 140Vpp. For voltages higher than 140Vpp, the loss starts increasing again.

4. Discussion

The measurements for the LC clad waveguides are only corrected for the contribution of the input and output grating couplers. We do not take into account the difference in loss between the parts of the waveguide covered (70%) and uncovered (30%) by the glass. Observation of the cell under the polarization microscope reveals that LC also covers the part of the waveguides uncovered by the glass plate. As a result we have the part of the waveguides uncovered by glass covered with LC oriented along the z-axis. The LC over this part of the waveguides does not reorient with increasing applied voltage whereas the LC in the glass covered part does. Accordingly, the loss we measure is a weighted average of the contribution from both parts of the waveguide according to the formula;

$$Loss = 0.3 Loss_{LC,uncovered} + 0.7 Loss_{LC,covered} \tag{3}$$

In order to verify this, we model the $W = 785$nm waveguide with an increasingly reoriented LC upper cladding layer. This is achieved by using n_{clad} for the cladding layer above the waveguide and varying the value of α from $0°$ to $70°$ in steps of $10°$. The case $\alpha = 0$ corresponds to the measurement at 0Vpp. When we apply (3) to the simulation results we obtain a plot similar to Fig. 7(a).
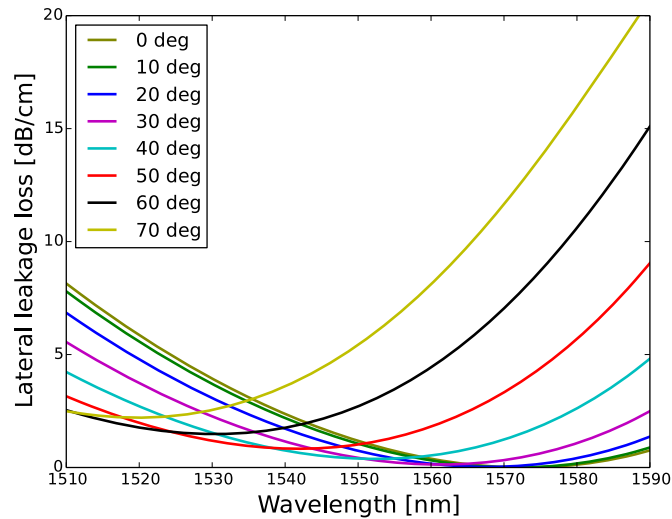

Fig. 8. Lateral leakage loss as a function of wavelength for increasing α.

Figure 8 exhibits the same features as Fig. 7(a); as α (i.e. the applied voltage) increases, the wavelength at which the minimum in lateral leakage loss occurs experiences a blue shift. The wavelength shift is accompanied by an increase in the lateral leakage loss. This only qualitatively explains the measurements for the LC clad waveguides. Closer inspection reveals that this effect alone cannot quantitatively explain the increase in loss. The LC molecules respond to an applied voltage by not only tilting (in the yz plane), but also twisting (in the xz plane). This results in fluctuations in the LC director profile along the length of the waveguide. Each LC director profile corresponds to a given phase-matching angle between the radiating slab TE mode and the guided TM-like mode. Since each phase-matching angle corresponds to a different magic wavelength, the measured loss is a weighted average of the loss corresponding to each of the different LC director profiles which occur along the length of the waveguide. The overall result is an increase in measured loss with increasing applied voltage.

The performance of the device can be improved by minimizing the effect of the defects generated by the sides. For low applied voltages, this can be achieved by increasing the separation between the waveguide and the sides. When a voltage is applied to the LC layer, the defects propagate through the cell. Given that defects in a LC cell typically extend over a distance comparable to the thickness of the cell, the scattering in the LC layer close to the waveguide increases with increasing applied voltage. Increasing the distance between the sides and the waveguide will also make it possible to achieve a greater reduction in the scattering with increasing voltage than achieved here.

The voltages mentioned above are quite high. The LC cells we fabricate have several dielectric layers between the two electrodes (see Fig. 3). The dielectric permittivity of silica, PMMA and LC in the KHz range is equal to 3.9, 2.6 and 5.1 (for low voltages, and 19.6 for high voltages). Accordingly, despite the fact that the LC layer is thicker than the other dielectric layers, the voltage drop over it is only a fraction of the total applied voltage. For low and high applied voltages this fraction is equal to about 40% and 15% of the applied voltage respectively. The problem of high applied voltages can be solved by doping the shallow-etched waveguide slab, so that it can be used as an electrode.

The method we propose for tuning the position of the leakage loss minima of LC clad shallow-etched waveguides opens up the possibility to have voltage-tunable reconfigurable single-mode optical interconnects (waveguides) operating over a wide band of wavelengths. As we show, such interconnects can be wider than other silicon photonic single-mode waveguides and hence potentially more fabrication tolerant. We have also demonstrated wavelength selective transmission with an extinction ratio of 20dB/cm. More sophisticated waveguide designs can be conceived that would increase the number of wavelengths which are efficiently transmitted through a single waveguide, and thus single-mode on-chip wavelength division multiplexing should be possible. Our work also opens up interesting possibilities for applications in which it is important to tune the loss of a signal. A high extinction Mach-Zehnder interferometer is an example of such an application. If you can balance the power exactly between the arms by trimming the loss (using the LC) in one arm, you can get higher contrast interference. It should also be noted that the power lost from the waveguide through the lateral leakage phenomenon is converted into coherent TE radiation. By controlling the rate of leakage along the waveguide, it is possible to achieve on-chip beam forming [18]. Our demonstration of dynamic reconfiguration of lateral leakage using LCs opens up the possibility for dynamic beam forming on-chip with applications in information imaging and sensing as well as information processing and signal routing.

5. Conclusion

We have demonstrated a new method for tuning the lateral leakage loss of TM-like modes in shallow etched LC clad SOI waveguides. We started out by measuring the leakage loss in an air-clad waveguide. We then proceed by giving details about how to incorporate a LC cladding on the waveguide. We then measure the leakage loss of the LC clad waveguides and find it to be comparable to the air-clad case. Finally, we also show that for a fixed wavelength, the leakage loss can be modulated by appropriately modulating the applied voltage.

Acknowledgments